


# Histologic Analysis with the Newly Designed Exoskeleton Seal<sup>®</sup> Stent-Graft in the Porcine Abdominal Aorta

Jung-Hoon Park<sup>1</sup> · Young Kwon Cho<sup>2</sup>  · Keun Her<sup>3</sup> · Yong Sun Jeon<sup>4</sup> · Jeong Ho Kim<sup>5</sup> · Tae-Seok Seo<sup>6</sup> · Myung Gyu Song<sup>6</sup>

Received: 5 March 2019 / Accepted: 3 June 2019 / Published online: 14 June 2019

© Springer Science+Business Media, LLC, part of Springer Nature and the Cardiovascular and Interventional Radiological Society of Europe (CIRSE) 2019

## Abstract

**Purpose** To investigate the technical feasibility of a novel exoskeleton Seal<sup>®</sup> stent-graft and analyze early histologic changes in the porcine abdominal aorta.

**Materials and Methods** Six pigs received an abdominal stent-graft (Group I), and six received an iliac branch stent-graft (Group II). Groups were subdivided as follows: Group Ia, which received three bifurcated main-body stent-grafts; Group Ib, which received three bifurcated main-body stent-grafts with both iliac graft-stents; Group IIa, which received three simple uni-iliac tapered stent-grafts; and Group IIb, which received three uni-iliac tapered tapered stent-grafts with right straight limb and left branched limb. Statistical analyses were performed with the Wilcoxon signed-rank test and mixed-model regression analysis.

**Results** The primary technical success rate (< 24 h) was 83% because of two acute thromboses in the lumen of the stented abdominal aorta immediately after stent-graft placement. At 4 weeks, late thrombosis occurred in two pigs. Higher mean neointimal hyperplasia areas (23.5% vs. 16.2%;  $P = .047$ ), neointimal hyperplasia thicknesses (545.5  $\mu\text{m}$  vs. 422.2  $\mu\text{m}$ ;  $P = .001$ ), and degrees of collagen deposition (2.71 vs. 2.33;  $P = .002$ ) were observed at the bare-metal stent-graft compared with the proximal exoskeleton portion of the stent-graft, with no significant differences between the patent and occluded groups or among the four types of stent-grafts.

**Conclusions** The exoskeleton stent-graft demonstrates 66% of patency rate during 1-month follow-up due to four cases of thromboses; however, the endothelialization on the junction of proximal graft showed no significant differences between the patent and occluded groups. Further studies should investigate long-term outcomes with prolonged neointimal hyperplasia.

✉ Young Kwon Cho  
ykchoman@naver.com

<sup>1</sup> Biomedical Engineering Research Center and Department of Radiology, Asan Medical Center, University of Ulsan College of Medicine, Seoul, Korea

<sup>2</sup> Department of Radiology, Kangdong Seong-Sim Hospital, Hallym University College of Medicine, 150 Seongan-ro, Gangdong-gu, Seoul 134-701, Korea

<sup>3</sup> Department of Thoracic Surgery, Soonchunhyang Bucheon University Hospital, Soonchunhyang University College of Medicine, Bucheon, Korea

<sup>4</sup> Department of Radiology, Inha University Hospital, Inha University College of Medicine, Incheon, Korea

<sup>5</sup> Department of Radiology, Gachon University Gil Hospital, Gachon University College of Medicine, Incheon, Korea

<sup>6</sup> Department of Radiology, Korea University Guro Hospital, Korea University College of Medicine, Seoul, Korea

**Keywords** Exoskeleton stent-graft · Animal studies · Porcine abdominal aorta · Thrombotic occlusions · Neointimal hyperplasia

## Introduction

Endovascular aortic repair (EVAR) of the abdominal aortic aneurysm (AAA) is widely accepted as an effective and less invasive treatment alternative to open surgical AAA repair [1]. Adequate early neointimal hyperplasia coverage

of the implanted stent-graft plays a crucial role both in the stability of the stent-graft and in the prevention of abnormal thrombosis. Theoretically, migration of endothelial cells from perigraft capillaries or circulating cells to arterial anastomoses is believed to play a major role in the stable healing process. This migration has been observed in animal models and is believed to be important in the early stages of healing after stent-graft implantation [2, 3].

The first commercially available stent-grafts for EVAR included various endoskeleton stent-grafts; however, several clinical trials have highlighted concerns regarding the complications associated with such devices, including an increased incidence of device migration, which has been reported to be 8.6% from 22 studies [4]. On the contrary, exoskeleton stent-grafts developed later have been known to be better fixation devices due to increasing radial force and improved embedding into the aortic wall compared with endoskeleton devices [5, 6].

At present, several manufacturers produce exoskeleton stent-grafts. The newly designed Seal<sup>®</sup> stent-graft (S & G Biotech Inc., Seongnam, Gyeonggi-do, Korea) is one such example, which has been modified for preclinical trials from the original endoskeleton Seal<sup>®</sup> stent-graft. We aimed to compare the inherent design and properties of the four types of exoskeleton device in terms of device usefulness for future clinical application after evaluation in normal porcine aorta, particularly the Group I device that has been designed to introduce exoskeleton design Seal<sup>®</sup> stent-graft in the field of EVAR and the Group II device that has been designed to introduce the iliac branching device (IBD) to spare the internal iliac artery and compare commercially available other IBDs [7, 8]. From this, the current study aimed to investigate early histologic changes in order to evaluate early device stability induced by the exoskeleton Seal<sup>®</sup> stent-graft in the porcine abdominal aorta.

## Materials and Methods

### Characteristics of the Newly Designed Seal<sup>®</sup> Stent-Graft

Four types of Seal<sup>®</sup> stent-grafts were designed and prepared according to the study protocol with nitinol wire frame and Dacron graft (Table 1). The newly designed exoskeleton Seal<sup>®</sup> stent-graft has four different structural features as follows: (1) the exoskeleton structure, with three parallel stent wires attached to the outer surface of the graft membrane of the main body in a zigzag manner; (2) the proximal bare-stent configuration, which was changed from hexagonal to octagonal for complete sealing; (3) the limb stent of the main-body stent-graft, which was changed to an ipsilateral 4-cm long limb and contralateral 2-cm

short limb (the old device included an ipsilateral short limb and contralateral long limb) for easier selection of the ostium of the contralateral limb; and (4) the two-step deployment of the main-body stent-graft through retrieval of the proximal constrained wire.

Group I stent-grafts were selected for the classic EVAR application with a supported uni-body, 7-cm bifurcated main-body stent-graft with a 3-cm uncovered proximal stent and a 4-cm ipsilateral long limb and 2-cm contralateral short limb. In Group Ia, the bifurcated main-body stent-graft was without the iliac limb graft-stent (Fig. 1A). In Group Ib stent-grafts, the bifurcated main-body stent-graft had a right flare iliac graft-stent and a left straight iliac graft-stent (Fig. 1B). Group II stent-grafts were selected for the application of the IBD, which has a uni-iliac main-body stent-graft with bilateral 3-mm tapered configuration and attached extension limb. In Group IIa, the uni-iliac tapered device had a single straight limb (Fig. 1C). In Group IIb, the uni-iliac main-body stent-graft had a right straight limb and a left branched limb (Fig. 1D). The wire thicknesses of the four types of stent-grafts were as follows: 0.178, 0.110, and 0.154 inches for the proximal bare-metal stent, proximal grafted main body, and middle-to-distal grafted main body to both the iliac limb graft-stents, respectively. The Group I device was loaded into a 15-F introducer sheath, and the Group II device was loaded into a 12-F introducer sheath. The size criteria of all prepared stent-grafts were decided based on computed tomography (CT) analysis at 1 week before the experiment with 10%–15% oversizing.

### Animal Study

This study and its protocols were approved by the committee for animal research at our institution and conformed with the US National Institute of Health Guidelines on the care and use of laboratory animals.

A total of 12 male Yucatan miniature pigs weighing 70–80 kg (Optipharm Corp., Osong, Korea) were randomized into two groups using computer-generated random numbers. Group I pigs ( $n = 6$ ) received three Group Ia and three Group Ib stent-grafts. Group II pigs ( $n = 6$ ) received three Group IIa and three Group IIb stent-grafts. Evaluation of inflammatory markers in the blood before and after stent-graft placement was not carried out.

All pigs were euthanized for histopathological examination by overdose of xylazine hydrochloride (Rompun<sup>®</sup>; Bayer, Seoul, Korea) 4 weeks after the stent-graft placement.

### Stent-Graft Placement Technique

After 24 h of fasting and under the supervision of a veterinarian, the pigs were pre-medicated with 50 mg of

**Table 1** Four types of newly designed exoskeleton stent-grafts for the porcine abdominal aorta

Group	Newly designed exoskeleton stent-graft							
	Main body				Iliac limb			
	Diameter (mm)		Length (mm)	Type	Diameter (mm)		Length (mm)	
	Proximal	Distal			Proximal	Distal		
Ia	16	16	70	–	–	–	–	
Ib	12	12	70	Right flare limb	8	12	70	
				Left straight limb	8	8	80	
IIa	12	6	70	Single straight limb	6	6	60	
IIb	14	8	40	Right straight limb	8	8	60	
				Left branched limb	6	6	20	

intramuscular ketamine, an endotracheal tube was placed, and anesthesia was administered through inhalation of 0.5%–2% isoflurane (Ifiran<sup>®</sup>; Hana Pharm. Co., Seoul, Korea) with oxygen, 1:1 (510 mL/kg/min).

All devices were implanted through cut-down exposure of the femoral artery. Pre-procedural abdominal aortography with the use of 8–10 mL/s of contrast medium (CM) (Omnipaque 300<sup>®</sup>; GE Healthcare, Cork, Ireland) introduced through a 5-F pigtail catheter (Cook Medical Inc.; Bloomington, IN, USA) was performed to measure the diameter and length of the abdominal aorta using quantitative coronary angiography (CAAS<sup>TM</sup>; Pie Medical, Maastricht, Netherlands). All devices were advanced and deployed at the distal abdominal aorta and the iliac artery by an experienced thoracic surgeon under fluoroscopic guidance after administration of 100 units/kg of heparin (Heparin<sup>®</sup>; Choongwae, Seoul, Korea). There were no cases of post-deployment ballooning of the prosthesis. Post-procedural abdominal aortography was performed to confirm the patency and location of the stent-graft.

### Image Analysis

Computed tomography was performed 1 week before the procedure with a 320-slice CT system (Aquilion One<sup>TM</sup>, Toshiba Medical Corp, Tokyo, Japan) to measure the size of the aorta. Scanning was performed from 2 cm above the diaphragm to the head of the femur. The injection rate was 8–10 mL/s, and the mean volume was 120 mL (range 80–145 mL). Follow-up CT and catheter aortography were performed 4 weeks after the procedure to verify the location of the stent-graft and detect procedure-related complications.

Analysis of CT images was performed with orthogonal two-dimensional coronal images and three-dimensional volume-rendered images generated via post-acquisition software (iNtution<sup>TM</sup>; TeraRecon, Foster City, CA, USA).

Aortography and CT images were analyzed by two experienced interventional radiologists based on the

following parameters: (1) patency of stent-graft; (2) intimal thickness at two points (proximal and mid-portion of the bare-metal stent and the junction between the bare-metal stent and the main-body stent-graft); (3) the presence, location, and extension of thrombosis; (4) the presence, location, and cause of device complication (migration, kinking, and fracture); and (5) the presence and locations of the collateral vessels around the stent-graft.

### Study Definitions

Primary technical success was defined as stent-graft deployment at the proper position, no conversion to open surgery, no device complication, and no animal death, based on the human recommendations of the Ad Hoc Committee for Standardized Reporting Practices in Vascular Surgery of the Society for Vascular Surgery/American Association for Vascular Surgery [9]. If intraluminal thrombosis was observed on the initial and follow-up aortography and CT, it was classified according to the onset, location, and flow limitation as acute (< 24 h) or chronic ( $\geq$  24 h), main-body stent-graft or iliac limb graft-stent, and occlusive or non-occlusive.

### Histologic Analysis

Surgical exploration of the stented aorta and the iliac artery was followed by gross examination to determine possible arterial injury after stent placement. Tissue samples were fixed in 10% neutral buffered formalin for 24 h, then embedded in paraffin and sectioned. The stented aorta was sectioned transversely in the middle portion of the bare-metal stent-graft and the proximal 1 cm of the graft portion of the exoskeleton main-body stent-graft (Fig. 2A). Slides were stained with hematoxylin and eosin (H&E) and Masson's trichrome (MT). Histologic evaluation using H&E involved calculating the neointimal hyperplasia-related percentage of the cross-sectional area using:  $100 \times (1 - [\text{stenotic stented area}/\text{original stented area}])$

**Fig. 1** The exoskeleton Seal<sup>®</sup> stent-graft prepared for this animal study. **A** A representative image and detailed schematic diagram of the main-body stent-graft of exoskeleton Seal<sup>®</sup> stent-graft prepared for animal study. **B** A representative image of the main-body stent-graft with bi-iliac graft-stent. **C** A representative image of the uni-iliac tapered main-body stent-graft. **D** A representative image of the uni-iliac tapered main-body stent-graft with single branched limb

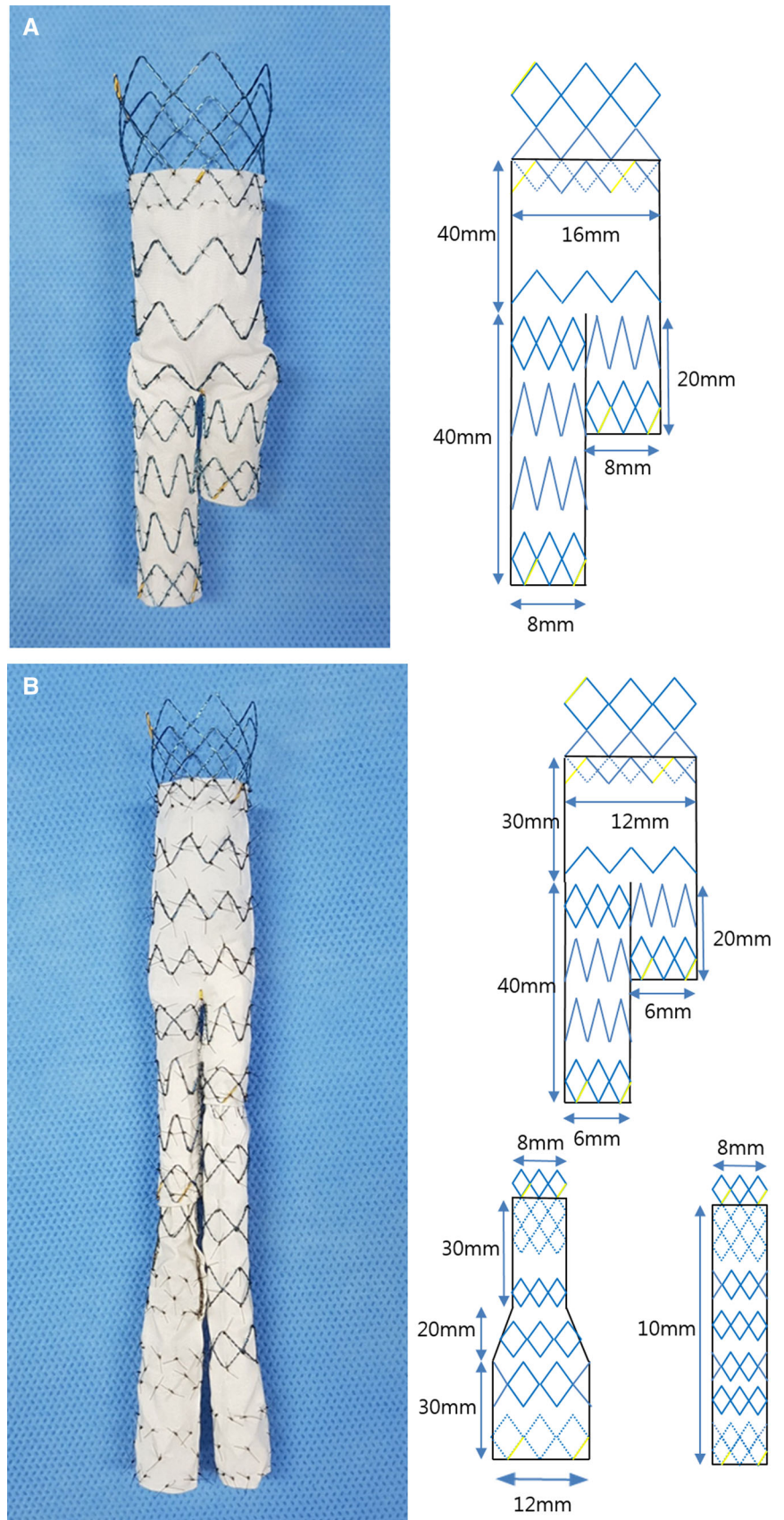
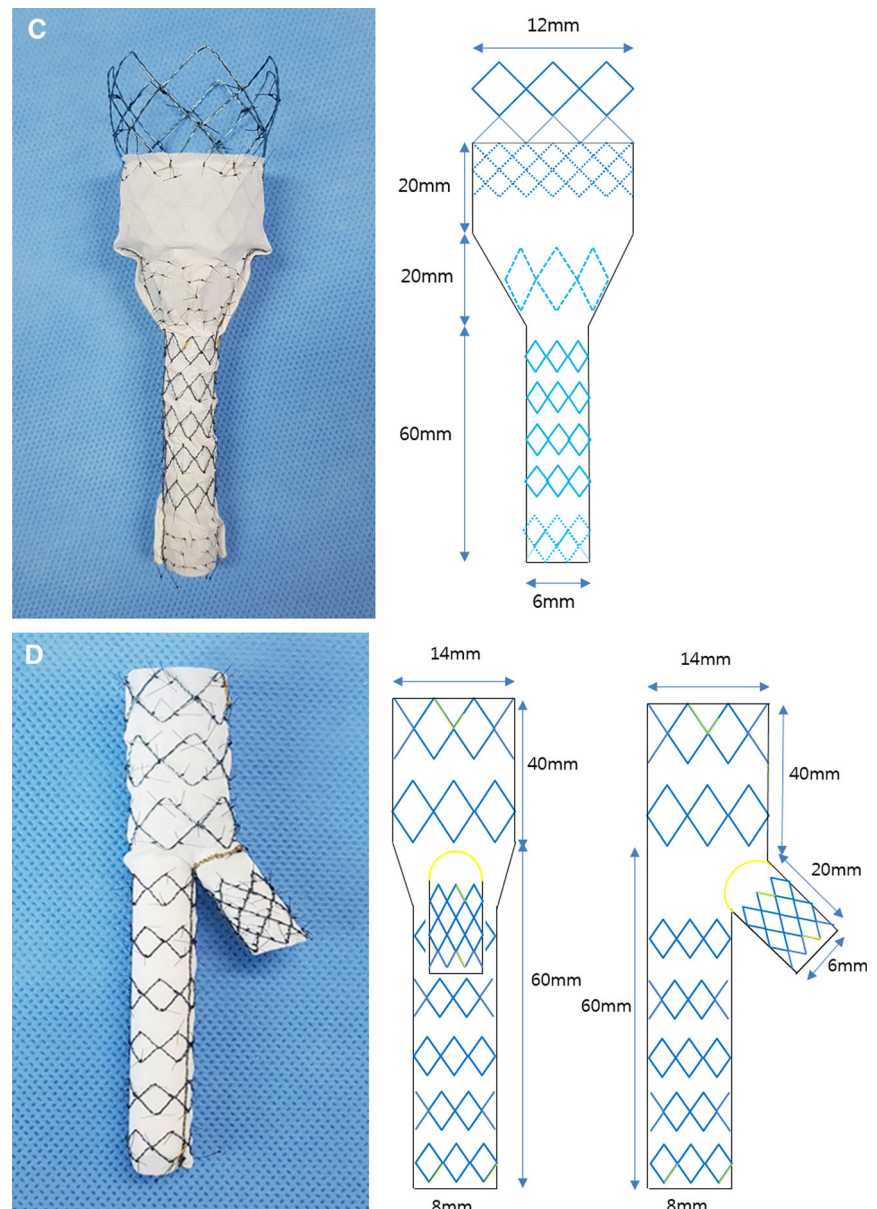


Fig. 1 continued



(Fig. 2B) and determining the thickness of neointimal hyperplasia and the degree of inflammatory cell infiltration. The degree of inflammatory cell infiltration was subjectively determined according to the distribution and density of inflammatory cells. The connective tissue area (as a percentage of the stent-graft area) and degree of collagen deposition in the neointimal hyperplasia over the stent-graft were determined using MT-stained sections. The degrees of collagen deposition and inflammatory cell infiltration were subjectively determined, where a score of 1 indicated mild, 2 indicated mild to moderate, 3 indicated moderate, 4 indicated moderate to severe, and 5 indicated severe. Average values for all variables were obtained by taking the mean of four points around the circumference. Histologic analysis was performed using a BX51

microscope (Olympus, Tokyo, Japan). Image-Pro Plus software (Media Cybernetics, Silver Spring, MD, USA) was used for the measurements. The stenotic stented area, original stented area, and thickness of neointimal hyperplasia were drawn manually, and the values were automatically calculated by the software [10]. The analyses of the histologic findings were assessed based on the consensus of three observers blinded to their group assignment.

### Statistical Analysis

The Wilcoxon signed-rank test was performed for statistical analyses of the neointimal hyperplasia differences in the two standard levels of stent-graft and the differences in

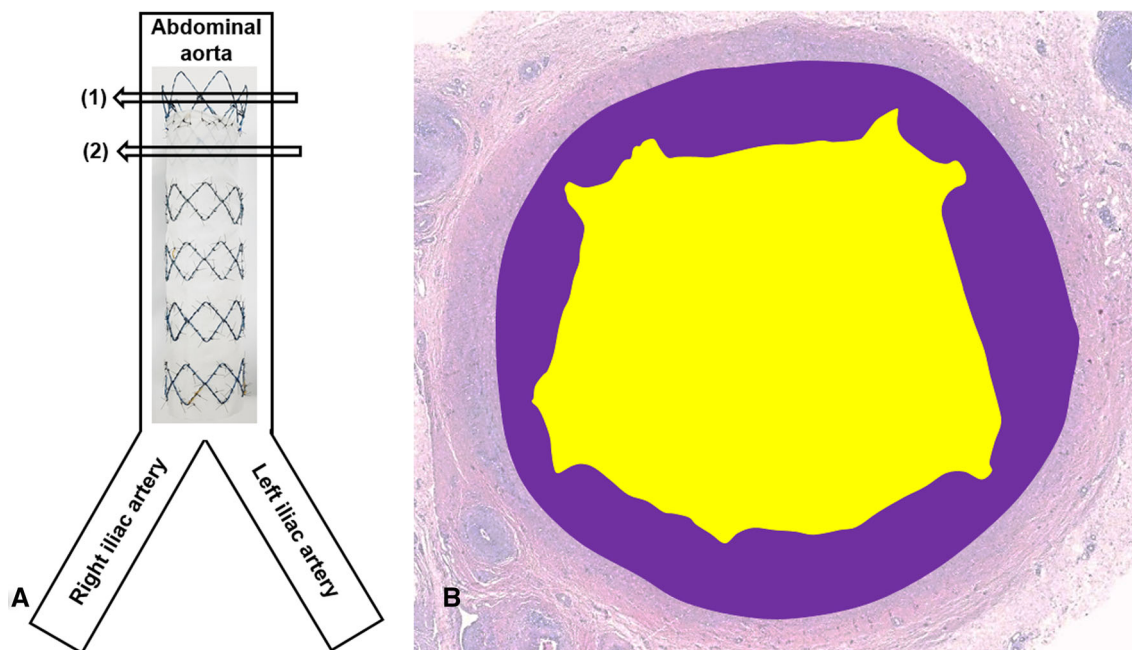


**Fig. 2** Location of tissue samples and histologic results. **A** A schematic image showing the location of tissue samples where the stent was present in (1) the middle portion of the bare-metal stent-graft and (2) the proximal 1 cm of the graft in the exoskeleton main-body stent-graft. **B** Histomorphometric methods of analysis of

histologic sections: stenotic stented area (yellow), original stented area (outer line of purple color), and neointimal hyperplasia (area of purple color). The percentage of neointimal hyperplasia area was calculated as  $100 \times (1 - [\text{stenotic stented area}/\text{original stented area}])$

each type of stent-graft using SPSS software (version 24.0; SPSS, Inc., Chicago, IL, USA). Mixed-model regression analysis was used to compare the neointimal hyperplasia differences in the patent stent-graft group and the occluded stent-graft group at the 4-week follow-up. A *P* value of  $< .05$  was considered statistically significant.

## Results

### Procedural Outcomes

Stent-grafts were technically successful in 10 out of 12 pigs (83%) without procedure-related complications. Two acute thromboses (one each in Groups Ib and IIb) occurred in the lumen of stented abdominal aorta immediately after stent-graft placement, which were confirmed by initial completion aortography (Fig. 3A, B). All stent-grafts were placed between the distal abdominal aorta and the proximal iliac artery regardless of the renal artery ostium, as the porcine abdominal aorta is very long compared with the usual length of stent-grafts. Two late thromboses (one each in Groups Ia and IIb) were identified at the 4-week follow-up CT. All pigs survived until the end of the study without further complications or additional anticoagulation.

### Image Findings

The average diameters of the abdominal aorta and the proximal iliac artery on preoperative CT performed 1 week before the experiment were as follows:  $13.4 \pm 1.7$  mm (median 12.9 mm; range 8.9–16.7 mm) for the suprarenal abdominal aorta,  $12.7 \pm 2.1$  mm (median 12.3 mm; range 8–15.9 mm) for the distal abdominal aorta, and  $7.5 \pm 1.3$  mm (median 7.8 mm; range 4.7–8.9 mm) for the iliac artery.

Radiology findings are summarized in Table 2. A total of eight stent-grafts in Groups I ( $n = 4$ ) and II ( $n = 4$ ) showed good patency in the lumen of the stent-grafts without graft complications; examples are shown in Fig. 4. Six of these eight stent-grafts showed a very thin circumferential low density along the inner wall of the stent-grafts in Groups I ( $n = 2$ ) and II ( $n = 4$ ). Two late occlusions of the stent-grafts were detected in the follow-up aortography and CT.

### Gross Specimen Findings

Results of the gross specimen inspection are summarized in Table 3. The four occluded stent-grafts and the eight patent stent-grafts were finally confirmed on the gross specimen inspection. The luminal surface of the eight stent-grafts with patent lumen was covered with glossy white thin

**Fig. 3** Results of Group Ib stent-grafts. The fluoroscopy image after main-body stent-graft placement (A) and completion aortography (B) show diffuse acute thrombosis (arrows) in the lumen of the Group Ib main-body Seal® stent-graft in the infrarenal porcine abdominal aorta



**Table 2** Radiological image findings on 4-week follow-up aortography and CT examination

Group	No.	Aortography				CT			
		Patency	Thrombosis	Collaterals	Graft complication	Patency	Thrombosis		
							Lumen	Graft wall <sup>b</sup>	Location
Ia	1	Patent	None	None	None	Patent	None	Present	(-)
	2	Occluded	Present	Present	None	Occluded	Total <sup>a</sup>	None	Main body
	3	Patent	None	None	None	Patent	None	None	(-)
Ib	7	Occluded	Present	Present	None	Occluded	Total <sup>a</sup>	None	Main body Both iliac limbs
	8	Patent	None	None	None	Patent	None	None	(-)
	9	Patent	None	None	None	Patent	None	Present	(-)
IIa	4	Patent	None	None	None	Patent	None	Present	(-)
	5	Patent	None	None	None	Patent	None	Present	(-)
	6	Patent	None	None	None	Patent	None	Present	(-)
IIb	10	Occluded	Present	Present	None	Occluded	Total <sup>a</sup>	None	Main body
	11	Patent	None	None	None	Patent	None	Present	(-)
	12	Occluded	Present	Present	None	Occluded	Total <sup>a</sup>	None	Main body

Total<sup>a</sup>: total thrombotic occlusion on the lumen of the stent-graft

Graft wall<sup>b</sup>: thin circumferential low attenuation along the inner surface of the main-body stent-graft or the iliac limb graft-stent

neointima along the full length of the stent-graft. The stent-graft occlusion was observed at the junction of the bare-metal stent and the grafted main body in all occluded stent-graft specimens ( $n = 4$ ).

**Histologic Findings**

Histologic findings are summarized in Table 4, and examples are shown in Fig. 5. Comparing the bare-metal portion of the stent-graft with the exoskeleton graft portion of the stent-graft, higher values were seen for the mean

**Fig. 4** Results of Groups Ib and IIa stent-grafts. **A** The completion angiography shows proper position and wide lumen of the Group Ib main-body Seal® stent-graft. **B** The completion angiography shows proper position and wide lumen of the Group IIa Seal® stent-graft and completely occluded left iliac artery by distal limb of uni-iliac stent-graft

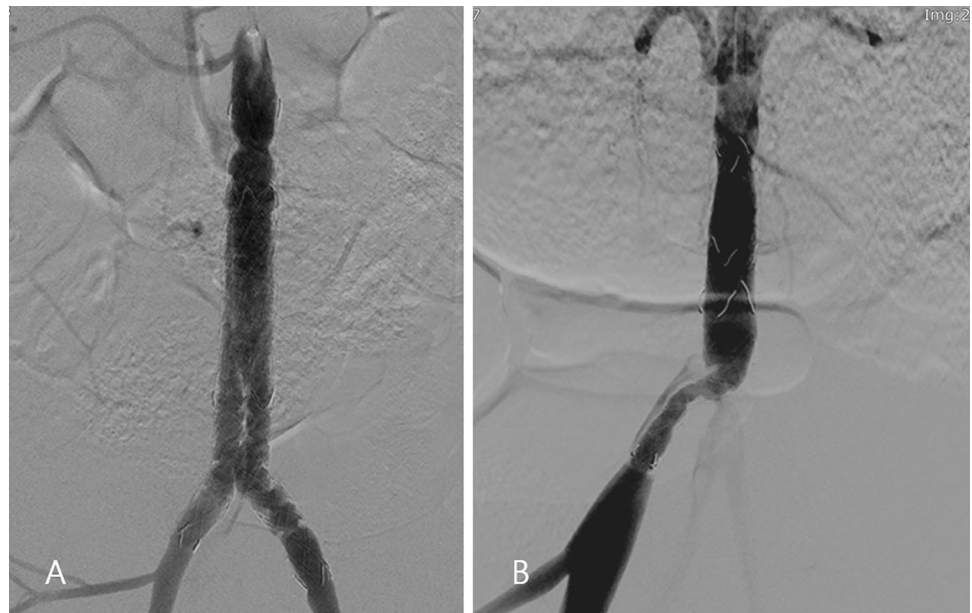


**Table 3** Results of gross specimen and histologic examinations of neointimal hyperplasia

Group	No.	Histologic examination of neointimal hyperplasia							
		Area of neointimal hyperplasia (%)		Thickness of intima to subintima ( $\mu\text{m}$ ) <sup>a</sup>		Degree of inflammatory cell infiltration <sup>b</sup>		Degree of collagen deposition <sup>c</sup>	
		Bare portion	Exoskeleton graft portion	Bare portion	Exoskeleton graft portion	Bare portion	Exoskeleton graft portion	Bare portion	Exoskeleton graft portion
Ia	1	17.8	17.1	430	386	1	2	3	2
	2	41.7	18.3	927	484	2	1	3	3
	3	45.7	27.4	833	638	2	1	3	2
Ib	7	18.8	12.9	566	417	1	2	2	2
	8	19.5	20.9	389	396	2	1	2	2
	9	12.4	12.2	421	406	1	2	2	2
IIa	4	25.8	15.5	518	423	1	2	3	2
	5	21.3	10.4	626	334	2	1	3	2
	6	22.2	13.9	541	342	2	2	3	2
IIb	10	12.1	10.4	393	449	2	2	2	2
	11	18.9	19.6	525	494	2	1	2	3
	12	26.2	9.9	378	298	1	2	2	2

Thickness of intima to subintima<sup>a</sup>: average value at four points (each 90° angle) of a cross section of the porcine aorta; degree of inflammatory cell infiltration<sup>b</sup>: average value at four points (each 90° angle) of a cross section of the porcine aorta; degree of collagen deposition<sup>c</sup>: average value at four points (each 90° angle) of a cross section of the porcine aorta

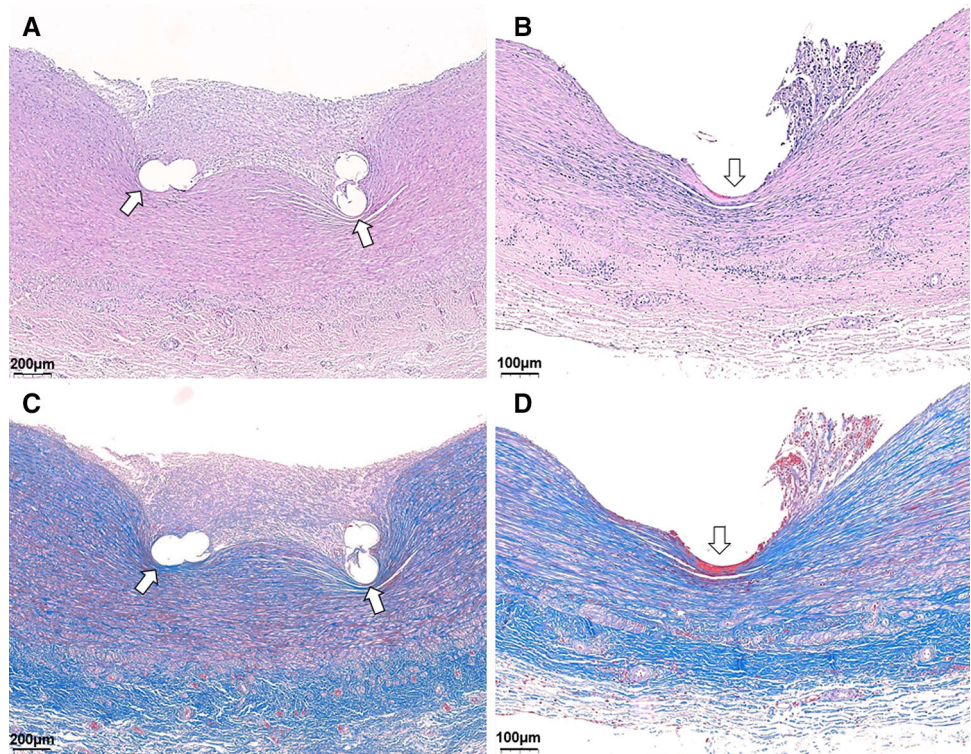
Grade 1 indicates mild; 2, mild to moderate; 3, moderate; 4, moderate to severe; 5, severe

**Table 4** Histologic findings after exoskeleton Seal® stent-graft placement in a porcine model

	Bare portion	Exoskeleton graft portion	<i>P</i> value
Neointimal hyperplasia area (%)	23.5 ± 10.4	16.2 ± 5.2	0.045
Thickness of the neointimal hyperplasia ( $\mu\text{m}$ )	545.5 ± 194.5	422.2 ± 140.4	0.001
Degree of inflammatory cell infiltration	1.67 ± 0.59	1.65 ± 0.53	0.856
Degree of collagen deposition	2.71 ± 0.62	2.33 ± 0.52	0.002



**Fig. 5** Histologic staining results. Representative microscopic images of the histologic slices obtained with hematoxylin and eosin (A, B) and Masson trichrome (C, D) stains. The neointimal hyperplasia area, thickness of neointimal hyperplasia, and degree of collagen deposition were significantly greater in the bare portion (A, C) compared with the proximal exoskeleton graft portion (B, D) of the stent-graft. Arrows = stent struts



percentage of the neointimal hyperplasia area (23.5% vs. 16.2%;  $P = .047$ ), mean thickness of the neointimal hyperplasia (545.5  $\mu\text{m}$  vs. 422.2  $\mu\text{m}$ ;  $P = .001$ ), and mean degree of the collagen deposition (2.71 vs. 2.33;  $P = .002$ ). However, the mean degree of inflammatory cell infiltration did not differ significantly between the two portions of the stent-graft (1.67 vs. 1.65;  $P = .856$ ).

There were no significant differences among the four groups in the percentage of neointimal hyperplasia ( $P = .928$ ), thickness of the neointimal hyperplasia ( $P = .024$ ), degree of collagen deposition ( $P = .332$ ), or degree of inflammatory cell infiltration ( $P = 0.908$ ).

There were no significant differences between the patent and occluded groups in the percentage of neointimal hyperplasia ( $P = .921$ ), thickness of the neointimal hyperplasia ( $P = .081$ ), degree of collagen deposition ( $P = .441$ ), or degree of inflammatory cell infiltration ( $P = .905$ ). The histologic findings in the patent and

occluded groups are summarized in Table 5, and examples are shown in Fig. 6.

### Discussion

In the present study, the newly designed exoskeleton Seal<sup>®</sup> stent-graft showed two unexpected acute and two late thrombotic occlusions; however, no evidence of graft complications, such as migration or graft kinking in all porcine aorta and no difference in intimal hyperplasia on the patent and occluded stent-grafts, was observed.

The technology of stent-grafts for the treatment of AAA has evolved with regard to device profile, fixation capability, and modular system construction. The metallic exo- or endoskeletons (stent frame at the outside or inside of the graft) have different advantages in terms of radial force, fixation capability, and proper neointimal proliferation. Exoskeleton stent frames might be associated with better

**Table 5** Histologic findings in patent and occluded groups after exoskeleton Seal<sup>®</sup> stent-graft placement in a porcine model

	Patent group (n = 8)	Occluded group (n = 4)	P value
Neointimal hyperplasia area (%)	19.9 ± 8.8	23.3 ± 9.9	0.921
Thickness of the neointimal hyperplasia ( $\mu\text{m}$ )	459.9 ± 167.2	531.9 ± 196.4	0.081
Degree of inflammatory cell infiltration	1.63 ± 0.52	1.72 ± 0.63	0.441
Degree of collagen deposition	2.52 ± 0.62	2.53 ± 0.57	0.905

Data are presented as mean ± standard deviation

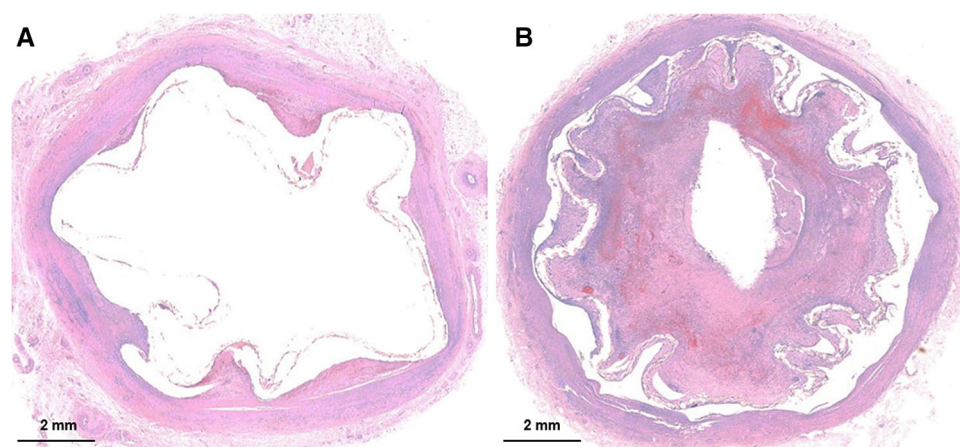


**Fig. 6** Representative microscopic images of the histologic slices obtained with hematoxylin and eosin staining in the patent (A) and occluded (B) groups at the proximal exoskeleton graft portion of the stent-graft. There were no significant differences between the patent

and occluded groups in terms of the percentage of neointimal hyperplasia, thickness of neointimal hyperplasia, degree of the collagen deposition, and degree of inflammatory cell infiltration

device fixation due to a stronger radial force, better embedding into the aortic wall, and better neointimal proliferation in the interstices of the stent [11]. For example, the Endurant device (Medtronic, Minneapolis, MN, USA) has an exoskeleton frame, which secures the proximal attachment site by friction and radial outward force of the exoskeleton stent wire [12]. Endoskeleton stent frames might have the advantage of better graft apposition to the aortic wall, better stretching out of the graft in accordance with the blood-flow stress and diameter of the aortic wall, less friction to the aortic wall, and less potential turbulence inside the stent-graft [13]. Kim et al. reported that the exoskeleton stent frame has advantages in terms of proper neointimal hyperplasia compared with the endoskeleton stent frame, since the exoskeleton stent-graft facilitates neointimal hyperplasia into the stent structure, which has been suggested to not occur in the endoskeleton structure from histologic examination [14, 15].

The endoskeleton Seal<sup>®</sup> stent-graft (S & G Biotech Inc., Seongnam, Gyeonggi-do, Korea) has been used in Korea since 2007. The endoskeleton design includes three parts: (1) a 5-cm bifurcated main-body stent-graft for 22–30 mm of the aorta diameter, which consists of a thin polyester bifurcated graft over a 3-stent frame connected by two bars positioned 2 cm from the uncovered proximal bare-stent, where the distal stent is attached to the ipsilateral 5-cm long limb and the contralateral 3-cm short limb; and (2) right iliac limb graft-stent and (3) left iliac limb graft-stent, which have a similar radial force and stent flexibility to those of other manufacturers (e.g., Cook and Gore companies) [16].

Among the commercially available stent-grafts, the Excluder (W. L. Gore & Associates, Inc., Flagstaff, AZ, USA), Endurant II (Medtronic, Minneapolis, MN, USA),

and Zenith Flex (Cook Medical, Bloomington, IN, USA) have exoskeleton stent frames, while the AFX2 (Endologix, Inc., Irvine, CA, USA) and INCRAFT (Cordis Corp, Bridgewater, NJ, USA) have endoskeleton stent frames [17]. In early 2017, S & G Biotech Inc. changed the Seal<sup>®</sup> stent-graft from an endoskeleton to an exoskeleton structure. The present animal study aimed to evaluate the prototype of the exoskeleton-framed Seal<sup>®</sup> stent-graft in a normal porcine aorta using four different types of stent-grafts.

In this study, no stent-graft migration was observed at the 4-week follow-up. Although longer follow-up periods would be beneficial, the homogenous intimal hyperplasia of the four types of stent-graft could contribute to early device stability. Comparisons of the inherent designs and properties of exoskeleton devices with endoskeleton devices could be an important aspect of clinical trials in order to establish whether this intimal hyperplasia contributes to device fixation. The occurrence of two acute thrombus formations immediately after stent-graft implantation might be associated with pleats and infoldings of the Dacron membrane of the Seal<sup>®</sup> stent-graft, which are likely to have contributed to larger stent-grafts for porcine aorta. The two delayed stent-graft occlusions might be associated with chronic intimal injury due to the increased radial force and thrombogenicity of the Dacron graft materials in the new device, as the device is larger than the native abdominal aorta and the Dacron graft is thicker and provides less graft apposition than a polytetrafluoroethylene graft, especially considering the smaller diameter of the porcine aorta [18, 19]. However, a recent study reported that exoskeleton-based devices exert increased friction on the tortuous aortic wall compared with endoskeleton-based devices [20].

The 1-month patency rate in this study was lower than that described by Kim et al. However, our histologic results revealed promising intimal hyperplasia over the stent-graft by prominent inflammatory cell migration and deposition of collagen over the stent-graft, which was observed consistently in all cases. This is supported by the finding that there were no significant differences between the patent and occluded groups with regard to the percentage and thickness of the neointimal hyperplasia, degree of collagen deposition, and degree of inflammatory cell infiltration [13]. This suggests that the cause of the stent-graft occlusions in this study may not be from intimal injury due to the radial force or oversizing of this device type to the porcine aorta, which was previously reported by van der Bas et al. [21].

This study had some limitations. First, the sample size was small and a heterogenous difference between the actual diameter of the aorta and the size of the stent-graft was observed. Because such a size difference can induce a high degree of intimal hyperplasia, due to stretching by an oversized stent-graft, demonstration of the clinical efficacy of the new device remains unclear. However, the degree of intimal hyperplasia showed no significant difference between the eight cases where patency was observed. Second, the prototype of the new device may have an unexpected stronger radial force than the old devices, despite careful manufacturing, which may have resulted in the four stent-graft occlusions in this study. Third, there were considerable technical difficulties in the procedure because of limited time under general anesthesia and the smaller size of the porcine aorta and iliac artery compared with humans. Fourth, a 1-month follow-up period, influenced by limitations in research funding, might be too short to evaluate a meaningful intima proliferation [3]. Fifth, direct comparison with devices from other manufacturers was not done, so we relied on reports from the current literature. Sixth, the study included no control groups for each type of stent-graft in the pathologic porcine aorta, which can limit our interpretations and cause difficulties in comparing the data of neointimal hyperplasia. Furthermore, correlative comparative analysis of neointimal hyperplasia between CT and histologic findings was limited by the resolution of the CT images.

## Conclusion

The new exoskeleton Seal<sup>®</sup> stent-graft resulted in four unpredictable acute and late thromboses in the normal porcine aorta. However, the endothelialization on the junction of bare-metal stent and proximal graft showed no significant differences between the patent and occluded groups. Thus, additional studies including histologic

examination, longer follow-up periods, larger sample sizes, and technical modification of stent-graft implantation are necessary to further evaluate this device.

**Funding** The study was supported by a Grant No. 2018-10 from the Kangdong Sacred Heart Hospital Fund.

## Compliance with Ethical Standards

**Conflict of interest** The authors declare that they have no conflict of interest.

**Ethical Approval** All applicable international, national, and/or institutional guidelines for the care and use of animals were followed.

**Informed Consent** For this type of study informed consent is not required.

**Consent for Publication** For this type of study consent for publication is not required.

## References

1. Parodi JC, Palmaz JC, Barone HD. Transfemoral intraluminal graft implantation for abdominal aortic aneurysms. *Ann Vasc Surg.* 1991;5:491–9.
2. Bashar AH, Kazui T, Terada H, Suzuki K, Washiyama N, Yamashita K, et al. Histological changes in canine aorta 1 year after stent-graft implantation: implications for the long-term stability of device anchoring zones. *J Endovasc Ther.* 2002;9:320–32.
3. Wu MH, Shi Q, Onuki Y, Kouchi Y, Sauvage LR. Histologic observation of continuity of transmural microvessels between the perigraft vessels and flow surface microostia in a porous vascular prosthesis. *Ann Vasc Surg.* 1996;10:11–5.
4. Spanos K, Karathanos C, Saleptsis V, Giannoukas AD. Systematic review and meta-analysis of migration after endovascular abdominal aortic aneurysm repair. *Vascular.* 2016;24:323–36.
5. Kent F, Ambler GK, Bosanquet DC, Twine CP, BSET (British Society for Endovascular Therapy). The safety of device registries for endovascular abdominal aortic aneurysm repair: systematic review and meta-regression. *Eur J Vasc Endovasc Surg.* 2018;55(2):177–83.
6. Steuer J, Lachat M, Veith FJ, Wanhainen A. Endovascular grafts for abdominal aortic aneurysm. *Eur Heart J.* 2016;37(2):145–51.
7. Maldonado TS, Mosquera NJ, Lin P, Bellosta R, Barfield M, Moussa A, et al. Gore Iliac Branch Endoprosthesis for treatment of bilateral common iliac artery aneurysms. *J Vasc Surg.* 2018;68:100–8.
8. Schneider DB, Matsumura JS, Lee JT, Peterson BG, Chaer RA, Oderich GS. Prospective, multicenter study of endovascular repair of aortoiliac and iliac aneurysms using the Gore Iliac Branch Endoprosthesis. *J Vasc Surg.* 2017;66:775–85.
9. Chaikof EL, Blankensteijn JD, Harris PL, White GH, Zarins CK, Bernhard VM, et al. Reporting standards for endovascular aortic aneurysm repair. *J Vasc Surg.* 2002;35:1048–60.
10. Li YD, Song HY, Kim JH, Woo CW, Park JH, Kim TH, et al. Evaluation of formation of granulation tissue caused by metallic stent placement in a rat urethral model. *J Vasc Interv Radiol.* 2010;21(12):1884–90.

11. Gorin DR, Arbid EJ, D'Agostino R, Yucel EK, Solovay KS, La Morte WW, et al. A new generation endovascular graft for repair of abdominal aortic aneurysms. *Am J Surg.* 1997;173:159–64.
12. Deery SE, Shean KE, Pothof AB, O'Donnell TFX, Dalebout BA, Darling JD, et al. Three-year results of the Endurant Stent Graft System Post Approval Study. *Ann Vasc Surg.* 2018;50:202–8.
13. Lambert AW, Budd JS, Fox AD, Potter U, Rooney N, Horrocks M. The incorporation of a stent-graft into the porcine aorta and the inflammatory response to the endoprosthesis. *Cardiovasc Surg.* 1999;7:710–4.
14. Kim YI, Choi YH, Chung JW, Kim HC, So YH, Kim HB, et al. Tissue responses to stent grafts with endo-exo-skeleton for saccular abdominal aortic aneurysms in a canine model. *Korean J Radiol.* 2014;15:622–9.
15. Kim HB, Choi YH, So YH, Min SK, Kim HC, Kim YI, et al. Tissue responses to endovascular stent grafts for saccular abdominal aortic aneurysms in a canine model. *J Korean Med Sci.* 2012;27:1170–6.
16. Kim JH, Cho YK, Seo TS, Song MG, Jeon YS, Han YM, et al. Clinical outcomes for endovascular repair of abdominal aortic aneurysm with the Seal stent graft. *J Vasc Surg.* 2016;64:1270–7.
17. Calero A, Illig KA. Overview of aortic aneurysm management in the endovascular era. *Semin Vasc Surg.* 2016;29:3–17.
18. Yavuz K, Geyik S, Pavcnik D, Uchida BT, Corless CL, Hartley DE, et al. Comparison of the endothelialization of small intestinal submucosa, dacron, and expanded polytetrafluoroethylene suspended in the thoracoabdominal aorta in sheep. *J Vasc Interv Radiol.* 2006;17:873–82.
19. Guidoin R, Chakfé N, Maurel S, How T, Batt M, Marios M, et al. Expanded polytetrafluoroethylene arterial prostheses in humans: histopathological study of 298 surgically excised grafts. *Biomaterials.* 1993;14:678–93.
20. Sincos IR, da Silva ES, Belczak SQ, Baptista Sincos AP, de Lourdes Higuchi M, Gornati V, et al. Histologic analysis of stent graft oversizing in the thoracic aorta. *J Vasc Surg.* 2013;58:1644–51.
21. van der Bas JM, Quax PH, van den Berg AC, van Hinsbergh VW, van Bockel JH. Ingrowth of aorta vascular cells into basic fibroblast growth factor-impregnated vascular prosthesis material: a porcine and human in vitro study on blood vessel prosthesis healing. *J Vasc Surg.* 2002;36:1237–47.

**Publisher's Note** Springer Nature remains neutral with regard to jurisdictional claims in published maps and institutional affiliations.